Letter

Electronic correlations influence on the anomalous constitutive law between the structure and spectra of hydrogen bonds

Rui Liu,[1] Xinrui Yang,[2] Famin Yu,[2] Depeng Zhang,[3,4] Lu Wang,[2] Ruhong Zhou,[5,6,7,*] and Zhigang Wang[1,2,4,†]

[1]*Key Laboratory of Material Simulation Methods & Software of Ministry of Education, College of Physics, Jilin University, Changchun 130012, China*

[2]*Institute of Atomic and Molecular Physics, Jilin University, Changchun 130012, China*

[3]*Normal School, Shenyang University, Shenyang 110044, China*

[4]*Institute of Theoretical Chemistry, College of Chemistry, Jilin University, Changchun 130023, China*

[5]*Institute of Quantitative Biology, College of Life Sciences, Zhejiang University, Hangzhou 310058, China*

[6]*Shanghai Institute for Advanced Study, Zhejiang University, Shanghai, China*

[7]*Department of Chemistry, Columbia University, New York, New York, USA*

(Received 21 February 2024; accepted 22 May 2024; published 25 July 2024)

Classical constitutive law between the structure and spectra has long been established in most physical processes and behaviors. Despite the emerging consensus, whether this law applies to microscopic systems adhering to quantum mechanics remains a fundamental and open question, due to limitations in even the most state-of-the-art experimental techniques. Here, we report an anomalous constitutive law of hydrogen bonds (X-H$\cdots Y$) using a benchmark *ab initio* method. Notably, a donor X-H bond shortening occurred simultaneously with an unexpected redshift and enhanced intensity in IR spectra. The reason for donor X-H bond shortening is attributed to both the slowly increasing attractive force from the acceptor Y atom and the increasing short-range repulsive forces from other protons attached to the approaching acceptor Y atom. Furthermore, neither eliminating vibrational mixing nor introducing various physical effects make vibrational spectra respond to X-H bond shortening. Other structural-characterization NMR spectra provide robust evidence for this anomalous law. This anomalous law is ascribed to the interplay of electronic correlations. Our Letter thus inspires a reassessment of paradigms, which broadens the scope of microscopic behavior for finer control.

DOI: 10.1103/PhysRevResearch.6.L032019

Constitutive laws comprise fundamental relations in which multiple physical quantities map to one another, with broad applications in physics [1–3], material science [4,5], and more. One important law is the relation between structure and spectra of X-H$\cdots Y$ hydrogen bonds [6,7], as it unravels long-standing enigma of microscopic behavior driven by subtle changes in the hydrogen bonding topology. The conventional physical picture of the constitutive law reveals that the formation of hydrogen bonds can either weaken the donor X-H bond, leading to X-H bond elongation with redshift (downshift) and enhanced intensity in IR spectra [8,9], or strengthen the X-H bond, causing its shortening with blueshift (upshift) and diminished intensity [10–13]. The former is commonly known as classical hydrogen bonds, while the latter is so-called improper hydrogen bonds. Much progress has been made since then in exploiting the physical origins behind these two types of hydrogen bonds, which have been attributed to charge transfer, Pauli repulsion, and so forth [14–17]. Some studies have derived the slopes between donor X-H stretching frequency and bond length of these two types of hydrogen bonds, ranging approximately -1.07 to $-2.50\,\mathrm{cm}^{-1}/0.0001$ Å [18–20]. Although debates and uncertainties about these studies still occur today, there is an emerging consensus on the overall reliability and importance of the constitutive law.

Phenomena in the observable macroscopic world obey constitutive laws, whereas the microscopic world is governed by the laws of quantum mechanics [21–23]. Given the intricacies of physical effects and experimental resolution limits, this may result in formidable challenges to the validity of the constitutive law when describing many-body physics. Note that a large amount of theoretical studies on the constitutive law were performed using density functional theory (DFT) with adjustable parameters and low-order electronic correlation methods such as second-order Møller-Plesset perturbation theory (MP2), and empirical force fields [9–20,24–28]. It is therefore more urgent than ever to reassess the reliability of the constitutive law of hydrogen bonds using benchmark methods. Given the resource consumption of benchmark calculations and the large size of typical liquids, the smaller microscopic intermolecular systems are undoubtedly the most suitable choice. For instance, water dimer not only exhibits the calculated feasibility but also serves as a fundamental

*Contact author: rhzhou@zju.edu.cn

†Contact author: wangzg@jlu.edu.cn

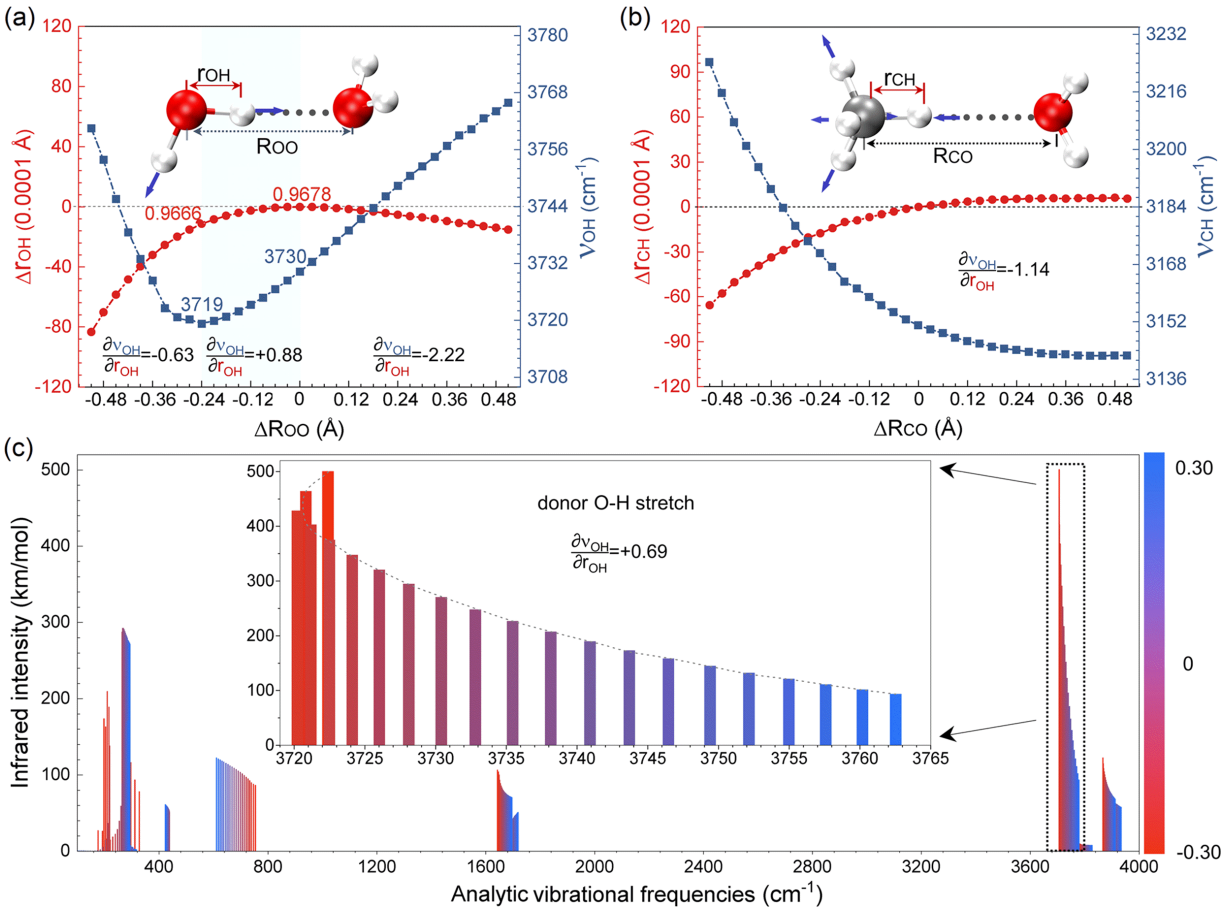

FIG. 1. Diagrams of structure and spectra. (a) Changes in donor O-H bond lengths (abbreviated as Δr_{OH}) and harmonic vibrational frequencies (abbreviated as ν_{OH}) versus O···O distance (abbreviated as R_{OO}) in water dimer. The cyan area denotes the anomalous region. (b) Changes in donor C-H bond lengths (abbreviated as Δr_{CH}) and harmonic vibrational frequencies (abbreviated as ν_{CH}) versus C···O distance (abbreviated as R_{CO}) in methane-water dimer. Optimal vibrational modes are plotted. (c) Infrared spectra with analytic second derivatives. Inner panel shows the infrared spectra of donor O-H stretch. The slopes between donor *X*-H bond length and analytic vibrational frequency according to the curves are presented.

mixture unit for liquid water [29,30], and constitutes the primary form in droplets and water-hydrophobic interfaces [31], which contributes to understanding complex behaviors of water clusters and overlayers on various surfaces. Therefore, analogous intermolecular hydrogen-bonded systems, such as hydrogen fluoride, hydrogen fluoride-water, and water-formaldehyde dimer, also hold typical significance.

In this Letter, we reassess the reliability of the constitutive law between structure and spectra of hydrogen bonds at the atomic level. Detailed calculations reveal that in certain systems, the contracting intermolecular distance at the atomic level causes simultaneously a donor *X*-H bond shortening and a surprising redshift with an enhanced intensity in IR spectra. Evidently, this result contradicts the expected blueshift and diminished intensity, thereby breaking down the empirical knowledge of constitutive law. Subsequent analyses of local vibrational properties, various physical effects, and nuclear magnetic resonance (NMR) spectra further support such anomalous law with more strong evidence. It turns out that the underlying physics of the anomalous behavior cannot be simply explained by a single reason, but rather arises from the intricate interplay of electronic correlations. As a result, these findings will provide a better understanding for microscopic properties in terms of empirical models and laws.

A prototype of hydrogen-bonded complexes, water dimer was first selected as our model system to comprehensively explore the constitutive law between the structure and spectra. Quantum simulations are carried out to refine donor O-H bond length and its stretching frequency as functions of intermolecular distance using the *ab initio* CCSD(T)/aug-cc-PVTZ (AUTZ) method. The comparison of present and previously measured geometries and spectra is given in Tables S1 and S2 of the Supplemental Material [32]. Despite subtle discrepancies from experimental observations due to the absence of nuclear quantum effect and anharmonicity, the present results are consistent with earlier *ab initio* values [19,33–35]. In Fig. 1(a), as two monomers approach each other to form the lowest-energy structure, the O-H covalent bond lengthens accompanied by the redshift of its stretching frequency, manifesting the cooperative effect of hydrogen bonds [36]. All data can be accurately fitted into a line with a slope of $-2.22\,\mathrm{cm}^{-1}/0.0001$ Å, which matches well with above-mentioned slope range observed in hydrogen-bonded complexes. Strikingly, when two monomers approach even

closer until O···O separation contracts by −0.24 Å, the O-H covalent bond shortens from 0.9678 to 0.9666 Å and simultaneously its stretching frequency redshifts from 3730 to 3719 cm^{-1} [light green shaded region in Fig. 1(a)]. Here, this results in a positive ratio of $+0.88\,cm^{-1}/0.0001$ Å, which appears counterintuitive. Subsequently, its behavior conforms to the constitutive law once again with further contraction. Note that that donor O-H bond shortening and blueshift are robust and reproducible, but at a higher negative slope of $-0.63\,cm^{-1}/0.0001$ Å than the general slope range. Therefore, a problem arises naturally, when the O-H bond length ranges 0.9678–0.9666 Å, as to whether the constitutive law might be invalid, at least in water dimer.

Faced with this problem, we performed additional studies for more hydrogen-bonded complexes, including homonuclear hydrogen fluoride dimer and water-formaldehyde dimer, as well as heteronuclear hydrogen fluoride-water dimer (Fig. S1 of the Supplemental Material). The rationality of structure selection is based on fully considering resource consumption of benchmark calculations, representativeness of physical models, and intricacies of physical effects, which has also been confirmed in previous work [37]. The results show that the heteronuclear hydrogen fluoride-water dimer follows constitutive law and exhibits a slope of $-1.14\,cm^{-1}/0.0001$ Å. Compared to those of water dimer, similar anomalous behaviors are also identified for both homonuclear hydrogen fluoride dimer and water-formaldehyde dimer. It was found that when two monomers approach closer, the F-H and O-H bonds shorten and the concomitant stretching frequencies redshift. As evident from this, their slopes within anomalous regions are positive at +1.79 and $+1.56\,cm^{-1}/0.0001$ Å, respectively. In addition to hydrogen-bonded systems, we extended our research to nonhydrogen-bonded complexes, including methane-water dimer and methane dimer. As depicted in Fig. 1(b), the C-H bond shortens and its stretching frequency blueshifts with the slopes of −1.14 and $-1.18\,cm^{-1}/0.0001$ Å. Thus, there is no such violation of the constitutive law in nonhydrogen bonded complexes.

To assess infrared intensity, another important physical quantity in constitutive law, we calculate the analytic vibrational spectra. Figure 1(c) presents a monotonic increase in the infrared intensity of donor O-H stretch from 94 to 501 km/mol as intermolecular separations contract, resulting in the hyperchromic effect. It is evident that even within the same contraction region, the anomalous behavior of analytic frequencies occurs with a positive slope of $+0.69\,cm^{-1}/0.0001$ Å, which is slightly lower than the $+0.88\,cm^{-1}/0.0001$ Å of numerical ones (Table S3 of the Supplemental Material). Especially noteworthy is the finding that unlike frequency shift, which only becomes anomalous within a certain contraction region, infrared intensity fails to reflect the change in *X*-H covalent bond length throughout the entire contraction process.

These findings have inspired us to seek the interaction force driving the anomalous behavior. The first point that needs to be explained is a continuum of behavior from lengthening to shortening in donor O-H bond lengths. As pointed out previously, the physical picture of compressed bulk water versus ice reveals that the donor O-H bond is less readily compressed than H···O separation [38]. As expected, the donor O-H bond becomes longer and weaker, while H···O separation becomes shorter and stronger, which is attributed to the cooperative effect of hydrogen bonds. It thus becomes more important to identify the interaction forces for O-H bond shortening. Subsequent explorations have indicated that compression force, Coulomb repulsion, and dislocation recovery force collectively determine bond length and strength [39]. In essence, these forces can be viewed as equivalent interactions on the bonded H proton, including the attractive force between a positive H proton and two negative O atoms, as well as the repulsive forces between positive H protons. Assuming each atom as an entity [Fig. 2(a)], the attractive forces exerting on bonded H proton can be fitted using the polynomial and exponential forms for

$$f^{\mathrm{attr}}_{\mathrm{donor\ O}} = f_1^0 + A_1 R_{\mathrm{OO}}, \tag{1}$$

$$f^{\mathrm{attr}}_{\mathrm{acceptor\ O}} = f_2^0 + A_2 e^{kR_{\mathrm{OO}}}, \tag{2}$$

where these two attractive forces are not macroscopic interactions, but rather modeled according to charge distribution, O-H bond length, and H···O separation at the atomic level. Among them, constants f_1^0, f_2^0, A_1, and A_2 are negative and k is positive. Additional details pertaining to the derivation of the above expression are provided in the text of Table S4 of the Supplemental Material. It is interesting to note that as two water monomers approach each other to form optimal water dimer, the attractive force from the donor O atom weakens, while that from the acceptor O atom strengthens, resulting in O-H bond elongation. This is consistent with the phenomenon previously found in bulk water and ice resulting from the cooperative effect. As water monomers come closer, the attractive force from the donor O atom decreases linearly in Eq. (1), while the attractive force from the acceptor O atom continues to increase but at an exponentially decelerating trend in Eq. (2). Meanwhile, the role of short-range repulsive forces from other H atoms (except for the H-bonding H proton) amplifies. These forces provide faithful explanations for resultant O-H bond shortening. Nevertheless, the reason and mechanism for the delayed response of vibrational spectra to such O-H bond shortening has not been revealed.

To eliminate the influence of vibrational mixing on the vibrational spectra [40–42], we analyzed local vibrational modes capable of capturing pure electronic effects, such as anharmonicity. Our analysis reveals that compared to normal ones, the anomalous constitutive law for local vibrational modes still occurs within the same contraction region [Fig. 2(b)]. At this point, the donor O-H bond shortens, accompanied by the redshift of local stretching frequency and the enhancement of infrared intensity. The slope of the local numerical mode at $+0.81\,cm^{-1}/0.0001$ Å is slightly higher than that of the analytic ones at $+0.73\,cm^{-1}/0.0001$ Å. A comparison with methane-water dimer implies a slope of $-0.98\,cm^{-1}/0.0001$ Å, which is higher than the $-1.14\,cm^{-1}/0.0001$ Å of normal ones. Besides, normal modes are decomposed into respective local mode contributions [Fig. 2(c)]. Normal modes are indeed dominated by donor O-H bond stretch, ∼80%. As stipulated in Fig. S2 and Table S5 of the Supplemental Material, the secondary contribution originates from the donor free O^1-H^4

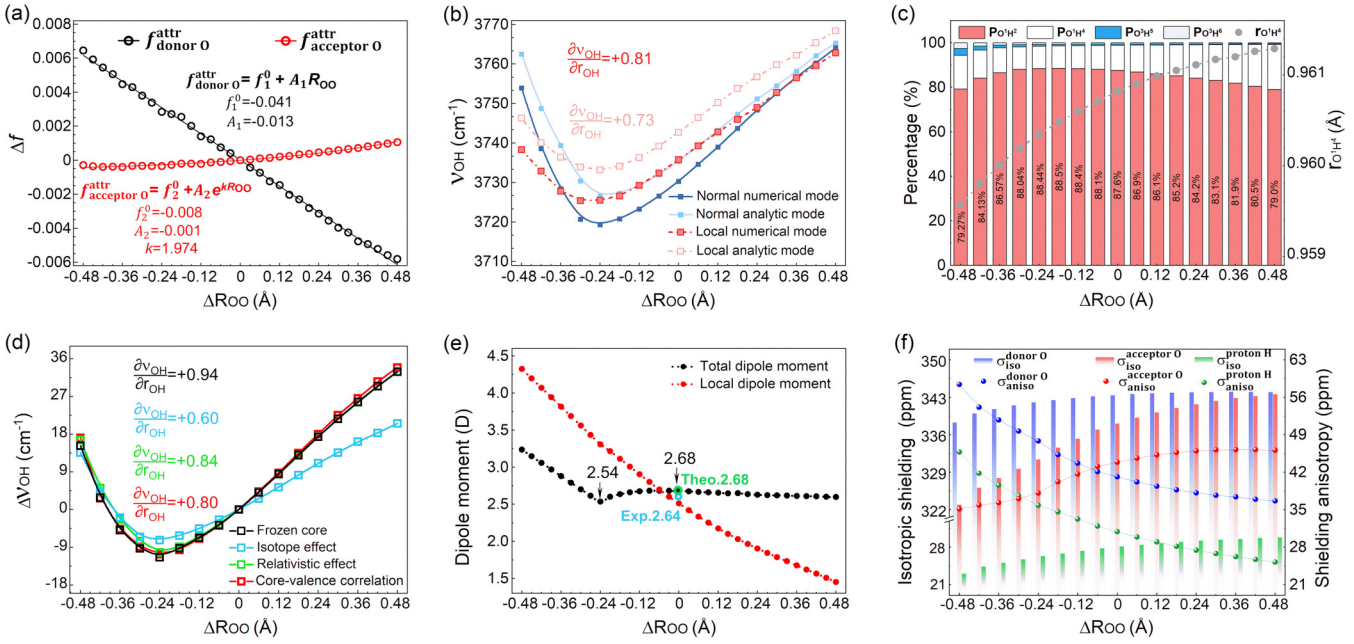

FIG. 2. (a) Attractive force analysis between positive H proton and two negative O atoms versus O···O distance, the polynomial, and exponential fitted according to the curves are presented. (b) Normal and local modes with numerical and analytic second derivatives. (c) Decomposition of normal mode of donor O-H stretch into the local mode contributions. The gray dotted line represents donor free O^1H^4 bond length. (d) Shifts in normal numerical vibrational frequencies affected by various physical effects, including frozen core approximation, isotope effect, relativistic effect, and core-valence correlation effect. The slopes between donor O-H bond lengths and stretching frequencies according to the curves are presented. (e) Total and local dipole moments. The light green and blue spheres represent previous *ab initio* calculated and experimental values (see, e.g., Refs. [26,37]). (f) NMR isotropic shielding and anisotropy of donor O atom, acceptor O atom, and H atom connecting hydrogen bonds (abbreviated as $\sigma_{\rm iso}^{\rm donor\ O}$, $\sigma_{\rm iso}^{\rm acceptor\ O}$ and $\sigma_{\rm iso}^{\rm proton\ H}$ and $\sigma_{\rm aniso}^{\rm donor\ O}$, $\sigma_{\rm aniso}^{\rm acceptor\ O}$ and $\sigma_{\rm aniso}^{\rm proton\ H}$).

bond, which also exhibits systematic shortening at shorter intermolecular separations. Recent studies indicated that the H-O-H bending mode is sensitive to hydrogen bonding interactions not yet obscured by vibrational mixing and correlates with the conventionally studied O-H stretching mode [43–45]. However, it cannot account for the delayed response of vibrational spectra (see Fig. S3 of the Supplemental Material).

In addition, various physical effects are evaluated to improve higher accuracy of vibrational spectra. From Fig. 2(d), it can be seen that taking into account the all-electron CCSD(T)/AUTZ level theory as reference, the inclusion of various physical effects does not alter the existence of anomalous constitutive law and even the anomalous region. It remains within the same contraction region (see Table S6 of the Supplemental Material). The slopes obtained with the inclusion of frozen core approximation, isotope effect, relativistic effect, and core-valence correlation effect are $+0.94$, $+0.60$, $+0.84$, and $+0.80\,\mathrm{cm}^{-1}/0.0001$ Å, respectively. Overall, these findings suggest that although various physical effects and vibrational mixing quantitatively influence vibrational frequency, anomalous constitutive law still occurs.

It is interesting to note that compared to vibrational frequency, the increase in infrared intensity cannot reflect O-H bond shortening throughout the entire contraction process. As noted earlier, infrared intensity is proportional to the squares of dipole moment derivatives [46,47]; both total dipole moment and local dipole moment of donor O-H bond are calculated [Fig. 2(e)]. The total dipole moment for water dimer is 2.68 D, which is equal to the low-order *ab initio* value and somewhat higher than the experimental value of 2.64 D [30,48], confirming the reliability of our calculations. A transition point of total dipole moment from decreasing to increasing is identified at contracting O···O separation of -0.24 Å (see Table S7 of the Supplemental Material). The transition point coincides well with vibrational frequency. Moreover, as expected from infrared intensity, there is a monotonic increase in the local dipole moment of the donor O-H bond, suggesting that the underlying physical quantity behind infrared intensity fails to capture O-H bond shortening as well.

Next, NMR spectra, as another structure-characterization approach of hydrogen bonds [49,50], were carried out. The NMR isotropic shielding and anisotropy tend to correlate with structure and vibrational properties [51–53]. As depicted in Fig. 2(f), there is a decrease in the isotropic shielding constants of donor O ($\sigma_{\rm iso}^{\rm donor\ O}$), proton H ($\sigma_{\rm iso}^{\rm proton\ H}$), and acceptor O ($\sigma_{\rm iso}^{\rm acceptor\ O}$) when two monomers come closer together, due to the deshielding effect. Notably, acceptor O is more sensitive to geometric changes, ranging 343.6–323.0 ppm. Compared with the monotonous decrease in isotropic shielding, the shielding anisotropies of donor O ($\sigma_{\rm aniso}^{\rm donor\ O}$) and proton H ($\sigma_{\rm aniso}^{\rm proton\ H}$) increase, whereas those of acceptor O ($\sigma_{\rm aniso}^{\rm acceptor\ O}$) decrease. Accordingly, proton H and donor O become more sensitive to geometric changes, ranging 25.2–45.8 and 36.7–58.4 ppm, respectively (see Tables S8 and S9 of the Supplemental Material). The results reported here are

cross-checked by calculating the parallel ($\sigma_{||}$) and perpendicular ($\sigma_{\perp}$) components. Overall, it is reasonable to speculate that NMR observations cannot identify accurately structure and vibrational properties at the atomic level.

To gain deeper insight into the electronic correlation mechanism, we analyzed the electrostatic potential (ESP). The ESP is a real physical property that can be ascertained through experimental means, such as diffraction technique [54]. The ESP minimum has been utilized to characterize lone pairs, facilitating the understanding of hydrogen bond directionality and strength [55]. It was found that as two water molecules approach each other, the sp^3-O lone pairs of the donor water molecule become markedly more negative, ranging −59.05 to −69.41 kcal/mol (see Fig. S4 of the Supplemental Material). Conversely, the sp^3-O lone pairs of acceptor water molecule exhibit a relative positive shift, ranging −40.14 to −30.62 kcal/mol. Interestingly, partial sp^3-O lone pairs delocalize to the O-H antibonding orbital [σ^*(O-H)], which mirrors the extent of electron donation from sp^3-O lone pairs to the σ^*(O-H). This result is further supported by the adaptive natural density partitioning (AdNDP) localized orbitals (see Fig. S5 of the Supplemental Material). The mutual penetration distance between ESP isosurfaces of two water monomers provides further insight into hydrogen bond strength. The mutual penetration distances increase with decreasing O···O separations, indicating the stronger hydrogen bonding interactions, which coincides with the ESP minimum. Furthermore, to visually discern the interaction nature accurately, the independent gradient model based on Hirshfeld partition (IGMH) is calculated. The IGMH map in Fig. 3(a) reveals that intramolecular hydrogen bonds are contributed by both hydrogen bonding interaction and steric hindrance, whereas intermolecular hydrogen bonds are contributed by van der Waals interaction and hydrogen bonding interaction. Inter- and intramolecular interactions become increasingly repulsive. This phenomenon could be observed from the comparison of the δg^{inter} and δg^{intra} (see Fig. S6 of the Supplemental Material). All δg^{intra} values are more positive than δg^{inter}, implying stronger repulsion interaction. As a result, subtle variations in certain factors could cause such noticeable impacts, making it challenging to identify a single electronic correlation mechanism for the anomalous constitutive law.

Finally, to simulate experimental hydrostatic contraction, geometric deformation was equivalently converted to the external pressure required [Fig. 3(b)]. This pressure can be defined as the negative partial derivative of the electronic energy (G) with regard to volume (V), and all of the data can be accurately fitted to a quadratic polynomial expressed as

$$P = -\frac{\partial G}{\partial V} = A + BV + CV^2. \tag{3}$$

a subsequent analytic fit that yields the applied pressure. The G represents the contributions of both attractive and repulsive forces to the energy [56,57]. The calculated results show that the anomalous region can be observed at an induced pressure in Eq. (3), ∼16.9 GPa, and can provide incentives for future experimental studies,

In summary, we have systematically investigated the constitutive law between the structure and spectra of hydrogen bonds. Given the experimental resolution limits for observing

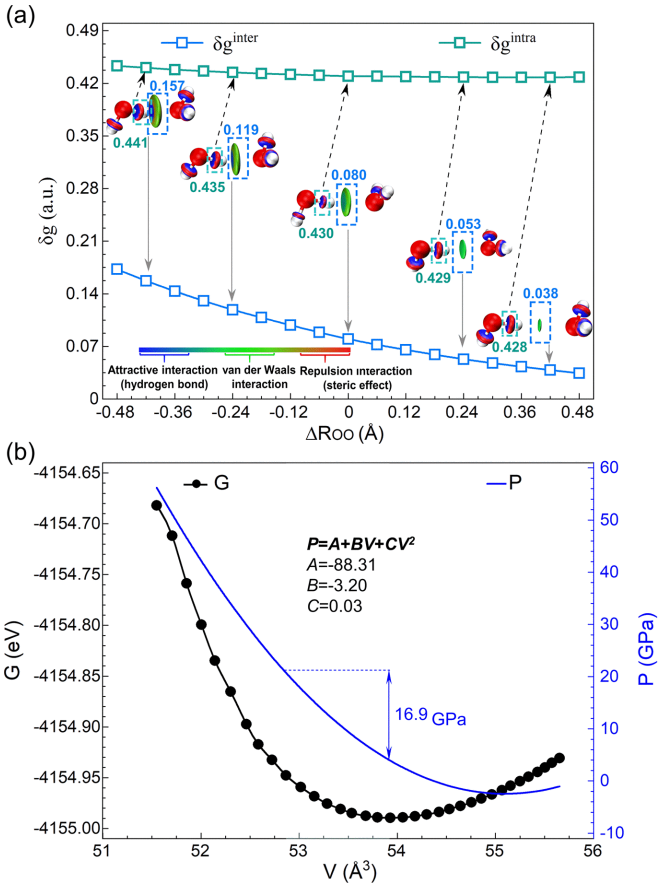

FIG. 3. Interaction analyses of IGMH types and simulated pressure. (a) sgn(λ_2)ρ colored isosurfaces of inter- and intramolecular differences of density gradient (δg^{inter} and δg^{intra}). The inter- and intramolecular colored areas are marked by blue and green squares. (b) Electronic energy (G) as a function of the volume (V). The cyan area indicates the anomalous region. The polynomial fitted according to the curves is presented.

microscopic structural changes with spectra and the inherent problems of DFT and low-order electronic correlation methods, there is an urgent need to employ benchmark methods for validating the constitutive law. High level CCSD(T) simulation results indicate that when two monomers approach each other at the atomic level, the X-H covalent bond can shorten under certain circumferences, while its stretching frequency redshifts and infrared intensity enhances surprisingly. This unexpected phenomenon challenges the reliability of widely accepted constitutive law. The reason for donor X-H bond shortening can be explained by interaction forces, in which attractive force from acceptor Y continues increasing but at exponential decelerating trend, while short-range repulsive forces from other H atoms (except for the H-bonding H proton) amplifies. However, neither eliminating vibrational mixing nor introducing various physical effects can result in an accurate response of the vibrational spectra to X-H bond shortening. Another structural-characterization NMR approach provides further evidence for this anomalous law. The reason for anomalous behavior is attributed to the interplay of electronic correlations, rather than a single factor.

This anomalous behavior may have benchmark implications for understanding the microscopic world and stimulate further exploration of research paradigm and experimental characterization techniques.

This work was supported by the National Key R&D Program of China (Grants No. 2021YFA1201200 and No. 2021YFF1200404), National Natural Science Foundation of China (Grants No. 11974136 and No. U1967217), and the Starry Night Science Fund of Zhejiang University Shanghai Institute for Advanced Study (Grant No. SN-ZJU-SIAS-003). Z.W. also acknowledges the assistance of the High-Performance Computing Center of Jilin University and National Supercomputing Center in Shanghai.

[1] J. Yarwood and G. N. Robertson, A new method of measuring the hydrogen bond stretching frequency $\nu\sigma$ of a complex in solution, Nature (London) **257**, 41 (1975).

[2] P. Jop, Y. Forterre, and O. Pouliquen, A constitutive law for dense granular flows, Nature (London) **441**, 727 (2006).

[3] M. Ohnaka, Nonuniformity of the constitutive law parameters for shear rupture and quasistatic nucleation to dynamic rupture: A physical model of earthquake generation processes, Proc. Natl. Acad. Sci. USA **93**, 3795 (1996).

[4] J. Standfuss, P. C. Edwards, A. D'Antona, M. Fransen, G. Xie, D. D. Oprian, and G. F. X. Schertler, The structural basis of agonist-induced activation in constitutively active rhodopsin, Nature (London) **471**, 656 (2011).

[5] H. D. Deng *et al.*, Correlative image learning of chemo-mechanics in phase-transforming solids, Nat. Mater. **21**, 547 (2022).

[6] S. A. C. McDowell and A. D. Buckingham, On the correlation between bond-length change and vibrational frequency shift in hydrogen-bonded complexes: A computational study of Y···HCl Dimers (Y = N_2, CO, BF), J. Am. Chem. Soc. **127**, 15515 (2005).

[7] X.-Z. Li, B. Walker, and A. Michaelides, Quantum nature of the hydrogen bond, Proc. Natl. Acad. Sci. USA **108**, 6369 (2011).

[8] E. Arunan, G. R. Desiraju, R. A. Klein, J. Sadlej, S. Scheiner, I. Alkorta, D. C. Clary, R. H. Crabtree, J. J. Dannenberg, P. Hobza, H. G. Kjaergaard, A. C. Legon, B. Mennucci, and D. J. Nesbitt, Definition of the hydrogen bond (IUPAC Recommendations 2011), Pure Appl. Chem. **83**, 1637 (2011).

[9] K. Ohno, M. Okimura, N. Akai, and Y. Katsumoto, The effect of cooperative hydrogen bonding on the OH stretching-band shift for water clusters studied by matrix-isolation infrared spectroscopy and density functional theory, Phys. Chem. Chem. Phys. **7**, 3005 (2005).

[10] B. J. van der Veken, W. A. Herrebout, R. Szostak, D. N. Shchepkin, Z. Havlas, and P. Hobza, The nature of improper, blue-shifting hydrogen bonding verified experimentally, J. Am. Chem. Soc. **123**, 12290 (2001).

[11] P. Hobza and Z. Havlas, Improper, blue-shifting hydrogen bond, Theor. Chem. Acc. **108**, 325 (2002).

[12] P. Hobza and Z. Havlas, Blue-shifting hydrogen bonds, Chem. Rev. **100**, 4253 (2000).

[13] S. N. Delanoye, W. A. Herrebout, and B. J. van der Veken, Blue shifting hydrogen bonding in the complexes of chlorofluoro haloforms with acetone-d6 and oxirane-d4, J. Am. Chem. Soc. **124**, 11854 (2002).

[14] G. Gilli and P. Gilli, *The Nature of the Hydrogen Bond: Outline of a Comprehensive Hydrogen Bond Theory*, International Union of Crystallography Monographs on Crystallography (Oxford University Press, New York, 2009).

[15] I. V. Alabugin, M. Manoharan, S. Peabody, and F. Weinhold, Electronic basis of improper hydrogen bonding: A subtle balance of hyperconjugation and rehybridization, J. Am. Chem. Soc. **125**, 5973 (2003).

[16] Y. Mao and M. Head-Gordon, Probing blue-shifting hydrogen bonds with adiabatic energy decomposition analysis, J. Phys. Chem. Lett. **10**, 3899 (2019).

[17] J. Joseph and E. D. Jemmis, Red-, blue-, or no-shift in hydrogen bonds: A unified explanation, J. Am. Chem. Soc. **129**, 4620 (2007).

[18] M. A. Boyer, O. Marsalek, J. P. Heindel, T. E. Markland, A. B. McCoy, and S. S. Xantheas, Beyond Badger's rule: The origins and generality of the structure–spectra relationship of aqueous hydrogen bonds, J. Phys. Chem. Lett. **10**, 918 (2019).

[19] S. S. Xantheas and T. H. Dunning Jr., Ab initio studies of cyclic water clusters $(H_2O)_n$, n = 1–6. I. Optimal structures and vibrational spectra, J. Chem. Phys. **99**, 8774 (1993).

[20] E. Miliordos, E. Aprà, and S. S. Xantheas, Optimal geometries and harmonic vibrational frequencies of the global minima of water clusters $(H_2O)_n$, n = 2–6, and several hexamer local minima at the CCSD(T) level of theory, J. Chem. Phys. **139**, 114302 (2013).

[21] Č. Brukner, Quantum causality, Nat. Phys. **10**, 259 (2014).

[22] P. J. Riggs, *Quantum Causality: Conceptual Issues in the Causal Theory of Quantum Mechanics* (Springer, New York, 2009), Vol. 23.

[23] J. Clarke, A. N. Cleland, M. H. Devoret, D. Esteve, and J. M. Martinis, Quantum mechanics of a macroscopic variable: The phase difference of a Josephson junction, Science **239**, 992 (1988).

[24] Y. Shi, Z. Zhang, W. Jiang, R. Wang, and Z. Wang, Infrared spectral-shift induced by hydrogen bonding cooperativity in cyclic and prismatic water clusters, J. Mol. Liq. **286**, 110940 (2019).

[25] I. Skarmoutsos, G. Franzese, and E. Guardia, Using Car-Parrinello simulations and microscopic order descriptors to reveal two locally favored structures with distinct molecular dipole moments and dynamics in ambient liquid water, J. Mol. Liq. **364**, 119936 (2022).

[26] E. Guardia, I. Skarmoutsos, and M. Masia, Hydrogen bonding and related properties in liquid water: A car–parrinello molecular dynamics simulation study, J. Phys. Chem. B **119**, 8926 (2015).

[27] S. S. Xantheas, Cooperativity and hydrogen bonding network in water clusters, Chem. Phys. **258**, 225 (2000).

[28] R. Vuilleumier and A. Seitsonen, Vibrational spectroscopies in liquid water: On temperature and coordination effects in Raman and infrared spectroscopies, Condens. Matter Phys. **26**, 33301 (2023).

[29] S. W. Benson and E. D. Siebert, A simple two-structure model for liquid water, J. Am. Chem. Soc. **114**, 4269 (1992).

[30] F. N. Keutsch and R. J. Saykally, Water clusters: Untangling the mysteries of the liquid, one molecule at a time, Proc. Natl. Acad. Sci. USA **98**, 10533 (2001).

[31] W. Fang, J. Chen, P. Pedevilla, X.-Z. Li, J. O. Richardson, and A. Michaelides, Origins of fast diffusion of water dimers on surfaces, Nat. Commun. **11**, 1689 (2020).

[32] See Supplemental Material at http://link.aps.org/supplemental/10.1103/PhysRevResearch.6.L032019 for the expressions used to compare previous experimental results and theoretical simulations, and their subtle discrepancies are due to the absence of nuclear quantum effect and anharmonicity.

[33] J. A. Odutola and T. R. Dyke, Partially deuterated water dimers: Microwave spectra and structure, J. Chem. Phys. **72**, 5062 (2008).

[34] T. R. Dyke, K. M. Mack, and J. S. Muenter, The structure of water dimer from molecular beam electric resonance spectroscopy, J. Chem. Phys. **66**, 498 (1977).

[35] T. R. Dyke, Group theoretical classification of the tunneling–rotational energy levels of water dimer, J. Chem. Phys. **66**, 492 (1977).

[36] K. Stokely, M. G. Mazza, H. E. Stanley, and G. Franzese, Effect of hydrogen bond cooperativity on the behavior of water, Proc. Natl. Acad. Sci. USA **107**, 1301 (2010).

[37] R. Liu, R. Wang, D. Li, Y. Zhu, X. Yang, and Z. Wang, An ab initio study on boundaries for characterizing cooperative effect of hydrogen bonds by intermolecular compression, Chin. Chem. Lett. **34**, 107857 (2023).

[38] C. Q. Sun, X. Zhang, and W. Zheng, The hidden force opposing ice compression, Chem. Sci. **3**, 1455 (2012).

[39] C. Q. Sun, Y. Huang, X. Zhang, Z. Ma, and B. Wang, The physics behind water irregularity, Phys. Rep. **998**, 1 (2023).

[40] J. Tse, D. Klug, C. Tulk, E. Svensson, I. Swainson, V. Shpakov, and V. Belosludov, Origin of low-frequency local vibrational modes in high density amorphous ice, Phys. Rev. Lett. **85**, 3185 (2000).

[41] E. Kraka, W. Zou, and Y. Tao, Decoding chemical information from vibrational spectroscopy data: Local vibrational mode theory, WIREs. Comput. Mol. Sci. **10**, e1480 (2020).

[42] W. Zou, R. Kalescky, E. Kraka, and D. Cremer, Relating normal vibrational modes to local vibrational modes with the help of an adiabatic connection scheme, J. Chem. Phys. **137**, 084114 (2012).

[43] T. Seki, K.-Y. Chiang, C.-C. Yu, X. Yu, M. Okuno, J. Hunger, Y. Nagata, and M. Bonn, The bending mode of water: A powerful probe for hydrogen bond structure of aqueous systems, J. Phys. Chem. Lett. **11**, 8459 (2020).

[44] T. Seki, S. Sun, K. Zhong, C.-C. Yu, K. Machel, L. B. Dreier, E. H. Backus, M. Bonn, and Y. Nagata, Unveiling heterogeneity of interfacial water through the water bending mode, J. Phys. Chem. Lett. **10**, 6936 (2019).

[45] C.-C. Yu *et al.*, Vibrational couplings and energy transfer pathways of water's bending mode, Nat. Commun. **11**, 5977 (2020).

[46] C. Ventalon, J. M. Fraser, M. H. Vos, A. Alexandrou, J.-L. Martin, and M. Joffre, Coherent vibrational climbing in carboxyhemoglobin, Proc. Natl. Acad. Sci. USA **101**, 13216 (2004).

[47] K. B. Wiberg and R. E. Rosenberg, A normal coordinate analysis and infrared intensities. Structure of the second rotamer, J. Am. Chem. Soc. **112**, 1509 (1990).

[48] J. K. Gregory, D. C. Clary, K. Liu, M. G. Brown, and R. J. Saykally, The water dipole moment in water clusters, Science **275**, 814 (1997).

[49] E. L. Ash, J. L. Sudmeier, R. M. Day, M. Vincent, E. V. Torchilin, K. C. Haddad, E. M. Bradshaw, D. G. Sanford, and W. W. Bachovchin, Unusual 1H NMR chemical shifts support (His) $C^{\varepsilon 1}$—H $\cdots$ O$=\!=$C H-bond: Proposal for reaction-driven ring flip mechanism in serine protease catalysis, Proc. Natl. Acad. Sci. USA **97**, 10371 (2000).

[50] J. A. Lukin, V. Simplaceanu, M. Zou, N. T. Ho, and C. Ho, NMR reveals hydrogen bonds between oxygen and distal histidines in oxyhemoglobin, Proc. Natl. Acad. Sci. USA **97**, 10354 (2000).

[51] E. Dib, I. M. Costa, G. N. Vayssilov, H. A. Aleksandrov, and S. Mintova, Complex H-bonded silanol network in zeolites revealed by IR and NMR spectroscopy combined with DFT calculations, J. Mater. Chem. A **9**, 27347 (2021).

[52] C. Guzmán-Afonso, Y. L.Hong, H. Colaux, H. Iijima, A. Saitow, T. Fukumura, Y. Aoyama, S. Motoki, T. Oikawa, T. Yamazaki, K. Yonekura, and Y. Nishiyama, Understanding hydrogen-bonding structures of molecular crystals via electron and NMR nanocrystallography, Nat. Commun. **10**, 3537 (2019).

[53] N. Tjandra and A. Bax, Understanding hydrogen-bonding structures of molecular crystals via electron and NMR nanocrystallography, J. Am. Chem. Soc. **119**, 8076 (1997).

[54] Y. Yang, H. Zhang, Z. Yuan, J. Q. Wang, F. H. Xiang, L. J. Chen, F. F. Wei, S. C. Xiang, B. L. Chen, and Z. J. Zhang, An ultramicroporous hydrogen-bonded organic framework exhibiting high C_2H_2/CO_2 separation, Angew. Chem. Int. Ed. **61**, e202207579 (2022).

[55] P. V. Bijina, C. H. Suresh, and S. R. Gadre, Electrostatics for probing lone pairs and their interactions, J. Comput. Chem. **39**, 488 (2018).

[56] B. Chen, R. Hoffmann, and R. Cammi, The effect of pressure on organic reactions in fluids—a new theoretical perspective, Angew. Chem. Int. Ed. **56**, 11126 (2017).

[57] T. Stauch, Quantum chemical modeling of molecules under pressure, Int. J. Quantum Chem. **121**, e26208 (2021).